Environment International 111 (2018) 362–371

Contents lists available at ScienceDirect

Environment International

journal homepage: www.elsevier.com/locate/envint

Proteomic evaluation of human umbilical cord tissue exposed to polybrominated diphenyl ethers in an e-waste recycling area

Minghui Li[a,1], Xia Huo[b,1], Yukui Pan[a], Haoxing Cai[a], Yifeng Dai[a], Xijin Xu[a,c,*]

[a] Laboratory of Environmental Medicine and Developmental Toxicology, Guangdong Provincial Key Laboratory of Infectious Diseases and Molecular Immunopathology, Shantou University Medical College, Shantou 515041, Guangdong, China

[b] Laboratory of Environmental Medicine and Developmental Toxicology, Guangzhou Key Laboratory of Environmental Exposure and Health, School of Environment, Jinan University, Guangzhou 510632, China

[c] Department of Cell Biology and Genetics, Shantou University Medical College, Shantou 515041, China

ARTICLE INFO

Keywords:
PBDEs
Umbilical cord
Proteomics
Fetal growth
E-waste

ABSTRACT

Parental exposure to polybrominated diphenyl ethers (PBDEs) is associated with adverse birth outcomes. This study aims to examine differentially-expressed protein profiles in umbilical cord tissue, derived from mothers exposed to PBDEs, and investigate candidate biomarkers to reveal the underlying molecular mechanisms. Umbilical cord samples were obtained from women residing in an electronic waste (e-waste) recycling area (Guiyu) and reference area (Haojiang) in China. The concentration of PBDEs in umbilical cord tissue was determined by gas chromatography and mass spectrometry (GC/MS). Isobaric tagging for relative and absolute quantification (iTRAQ)-based proteomic technology was conducted to analyze differentially-expressed protein profiles. The total PBDE concentration was approximately five-fold higher in umbilical cords from Guiyu than from Haojiang (median 71.92 ng/g vs. 15.52 ng/g lipid, $P < 0.01$). Neonatal head circumference, body-mass index (BMI) and Apgar1 score were lower in Guiyu and negatively correlated with PBDE concentration ($P < 0.01$). Proteomic analysis showed 697 proteins were differentially expressed in the e-waste-exposed group compared with the reference group. The differentially-expressed proteins were principally involved in antioxidant defense, apoptosis, cell structure and metabolism. Among them, catalase and glutathione S-transferase omega-1, were down-regulated, and cytochrome c was found to be up-regulated, changes which were further verified by enzyme-linked immunosorbent assays. These results suggest that an antioxidant imbalance and cell apoptosis in the umbilical cord following PBDE exposure is associated with neonatal birth outcomes.

1. Introduction

Electronic waste (e-waste) has become a global environmental health problem due to the rapid development of electronic technology (Ogunseitan et al., 2009; Heacock et al., 2016). Guiyu, a town with large-scale e-waste processing in southern China, is one of the largest e-waste sites in the world (Huo et al., 2007; Wu et al., 2010). Informal e-waste dismantling and recycling results in release of various toxic chemicals, including heavy metals, polychlorinated biphenyls (PCBs), and polybrominated diphenyl ethers (PBDEs), into the air, water and soil, and has caused severe health problems (Huo et al., 2007; Leung et al., 2007; Wu et al., 2010; Xu et al., 2013, 2014, 2015; Zhang et al., 2014). PBDEs are a group of brominated flame retardants that have been extensively used in various consumer products, such as electronic devices, construction materials, textiles and family furniture (Eskenazi et al., 2013; McDonald, 2002). PBDEs are easily released into the environment during e-waste dismantling, and affect human populations by entering the body via inhalation, ingestion, and dermal contact (Abdallah and Harrad, 2014; Darnerud et al., 2001; Sjodin et al., 2003). Due to their highly lipophilic properties, PBDEs are prone to accumulate in mothers and fetuses, mainly in fatty tissue and breast milk (Ma et al., 2012), umbilical cord blood (Zhao et al., 2016), placenta and fetal membranes (Miller et al., 2009; Solomon and Weiss, 2002; Wu et al., 2010). Since the chemical structure is similar to thyroid hormones and PCBs, PBDEs are inclined to disrupt the thyroid endocrine system (Zheng et al., 2017), and cause altered thyroid hormone homeostasis and neurotoxicity (Chen et al., 2014). Previous studies indicate prenatal exposure to high-levels of PBDEs is related to adverse neonatal birth outcomes and neurodevelopmental effects (Eskenazi et al., 2013; Wu et al., 2010).

* Corresponding author at: Laboratory of Environmental Medicine and Developmental Toxicology, Shantou University Medical College, Shantou 515041, Guangdong, China.
E-mail address: xuxj@stu.edu.cn (X. Xu).

[1] These authors contributed equally to the work.

https://doi.org/10.1016/j.envint.2017.09.016
Received 29 May 2017; Received in revised form 17 August 2017; Accepted 19 September 2017
Available online 21 November 2017

Proteomics is a potent method for detecting global changes in protein expression and identifying potential biomarkers that respond to environmental stressors (Bradley et al., 2002; Martyniuk et al., 2012; Zhang et al., 2012). Studies on the proteomic responses, following PDBE exposure, have been investigated in neonatal mouse brain striatum and hippocampus (Alm et al., 2006), rat cerebellum and hippocampus (Kodavanti et al., 2015), rat neural stem/progenitor cells (Song et al., 2014), *Mytilus galloprovincialis* (Ji et al., 2013) and human umbilical vein endothelial cells (Kawashiro et al., 2009), but have been conducted by conventional proteomics analysis involving two-dimensional electrophoresis (2-DE) combined with tandem mass spectrometry. In our previous study, we performed 2-DE technology to characterize the differential proteomic expression of human placenta and fetal development following e-waste lead and cadmium exposure in utero (Xu et al., 2016a). Isobaric tags for relative and absolute quantification (iTRAQ) proteomics coupled with liquid chromatography-tandem mass spectrometry (LC-MS/MS), which can analyze and quantify up to eight phenotypes with high resolution, has been commonly used to investigate mechanisms of chemical toxicity combined with altered protein expression profiles under chemical contaminant stress (Martyniuk et al., 2012; Ross et al., 2004).

The umbilical cord is not only responsible for the transport of nutrients and oxygen between fetus and mother, but also an ideal source of stem cells in tissue engineering and regenerative medicine (Chen et al., 2013). Xenobiotics are prone to accumulate in umbilical cord tissue during blood transportation and can cause varying degrees of damage to the structure and tissue of the umbilical cord. For instance, lead acetate has a toxic effect on the self-renewal, multipotent differentiation potential and hematopoiesis-promoting function of umbilical mesenchymal stem cells, and PBDEs cause oxidative stress in human umbilical vein endothelial cells (Charnley and Putzrath, 2001; Kawashiro et al., 2009; Sun et al., 2012; Zeng et al., 2014). However, the underlying mechanism of its effects remains unclear. Until now, no studies have investigated the effects of in utero PBDE exposure on protein expression profiles in the umbilical cord, and the correlation between umbilical PBDE exposure and fetal growth. Given the critical role of the umbilical cord in fetal growth and tissue medicine, we sought to examine the differentially-expressed protein profiles in umbilical cords from mothers exposed to PBDEs, and screen for biomarkers of its effects. In the current study, we applied an iTRAQ-based proteomic approach to investigate altered protein expression profiles of human umbilical cord tissue exposed to PBDE. This is the first study to examine the relationship between health risks of the neonate and PBDE levels in umbilical cord tissue from an e-waste recycling area. We focus on 3 differentially-expressed proteins, catalase (CAT), glutathione S-transferase omega-1 (GSTO1) and cytochrome c (Cyt c) in umbilical cord. These proteins involve antioxidant defense and cell apoptosis, which may affect fetal development and growth (Kawashiro et al., 2009). Our results may provide new insight for toxicity health risks of prenatal PBDE exposure on fetal development and growth by the novel proteomics.

2. Materials and methods

2.1. Study population

A total of 300 healthy pregnant women were recruited from a local hospital in both Guiyu and Haojiang between March and August 2012. Prior to enrollment, all participants answered a detailed questionnaire involving information covering maternal age, maternal weight and height, prenatal maternal smoking and drinking, education, father smoking, pregnancy complications, residential history and distance from an e-waste recycling site. Neonatal birth outcomes, including birth weight, body length and head circumference, were measured by medical professionals after delivery, and information was obtained from hospital records. The study protocol was approved by the Human Ethics Committee of Shantou University Medical College. Umbilical cord tissue samples were collected immediately following delivery by medical professionals. All tissue samples were taken from the neonatal side of the umbilical cord. After rinsing with cold sterile phosphate-buffered saline, samples were immediately frozen in liquid nitrogen, and then stored at − 80 °C until analysis.

2.2. Determination of PBDEs in umbilical cord tissue

Chemical analysis of PBDEs in umbilical cord tissue was with slight modifications of the procedure described in previous studies (Kawashiro et al., 2008; Xu et al., 2015). A PBDE standard mixture solution containing BDE-17, -28, -47, -66, -71, -85 -99, -100, -138, -153, -154, -183, -190, and -209, and individual standards BDE-15 and BDE-77, were purchased from AccuStandard (New Haven, CT, USA). BDE-15 and BDE-77 were used as internal and recovery standards, respectively. A 500 mg umbilical cord tissue sample was first extracted three times by addition of 10 mL of a 2:1 acetone/hexane solution and homogenizing for 1 min using a Pro200 homogenizer (Pro Scientific, USA). The supernatant was transferred and filtered through pre-cleaned (hexane) glass wool and anhydrous sodium sulfate. After concentrating to approximately 2 mL with a water bath, 20% of the extract was used for lipid gravimetric determination. The rest was filtered through a florisil glass column to remove lipids (lipid-adjusted PBDE concentration was used in the data analysis), then eluted with hexane for cleanup. The extract was concentrated to 1 mL under nitrogen for further cleanup with a multilayer silica gel column (1 g anhydrous sodium sulfate, 1 g of neutral silica, 1 g of basic silica, 3 g of acidic silica, 1 g of neutral silica, 1 g anhydrous sodium sulfate). The extracts were eluted with 50 mL dichloromethane, and then evaporated under a nitrogen stream until dryness, and resolubilized in 50 μL hexane. BDE-15 was used as the internal injection standard for analysis by gas chromatography/mass spectrometry (GC/MS). Samples were ultimately analyzed with an Agilent 7890A-5975C GC/MS (Agilent Technologies, America) with a negative chemical ion source.

For every ten samples, a solvent blank and a procedural blank were processed to make sure that samples were not contaminated. Instrumental accuracy was determined 7 times by constantly quantifying the minimum concentration of standard solution for the calibration curve. Relative standard deviation (RSD%) (tri-deca-BDE) was within 0.40%–4.00%. The limits of detection (LOD) (signal/noise of 3) was defined as three times the standard deviation (SD) of the method blanks analyzed in parallel with the study samples in 10 μL hexane (in the absence of detectable blanks) and ranged from 0.011 to 0.034 ng/mL for tri- to nona-BDE, and 0.070 ng/mL for BDE-209. The ten-point calibration curves showed excellent linearity ($r^2 > 0.999$). For recovery, a spiked sample with surrogate was determined for each batch. The average recoveries for surrogate standard ranged from 81%–95%.

2.3. Protein preparation, digestion, and labeling with iTRAQ reagents

Twenty-four umbilical cord tissues (twelve from the e-waste-exposed group and twelve from the reference group) were separated into three replicates for proteomic analysis, each replicate included eight samples (four samples/group). All samples with no birth complications and no birth defects, and pregnant women who smoked were excluded. From each of the 24 individual umbilical tissues, 100 mg was homogenized with lysis buffer (8 M urea, 40 mM Tris-HCl with 1 mM PMSF, 2 mM EDTA and 10 mM dithiothreitol, pH 8.5) and two magnetic beads (diameter 5 mm) were used to extract in a 1.5 mL centrifuge tube. The mixtures were placed into a Tissue Lyser for 2 min at 50 Hz torelease proteins. After centrifugation at 25,000*g* and 4 °C for 20 min, the supernatant was transferred to a new tube, reduced with 10 mM dithiothreitol at 56 °C for 1 h and alkylated with 55 mM iodoacetamide in the dark at room temperature for 45 min. Following centrifugation at 32,000*g* and 4 °C for 20 min, the supernatant was removed and

transferred into Eppendorf tubes and stored at −80 °C until further processing. The protein concentrations were measured with a Bradford kit according to the manufacturer's protocol.

Each 100 μg protein sample was denatured, reduced and blocked according to the iTRAQ 8-plex manufacturer's protocol (Applied Biosystems, USA). Briefly, tryptic digestion (Promega, USA) was performed at a protein: trypsin ratio of 30:1 and incubation at 37 °C overnight. The peptides were then desalted with a Strata X C18 column (Phenomenex, USA) and vacuum-dried. Peptides were reconstituted in 0.5 M TEAB, and labeled using the 8-plex iTRAQ reagents according to the manufacturer's instructions (Applied Biosystems, USA). Briefly, exposed group peptides were labeled with iTRAQ tags 113, 114, 115 and 116, and the reference peptides were labeled with tags 117, 118, 119 and 121, respectively. The labeled peptides with different reagents were combined and desalted with a Strata X C18 column and dried by vacuum centrifugation.

2.4. Strong cation exchange chromatography fractionation and LC-MS/MS analysis

Peptides were separated on an LC-20AB high-performance (HPLC) pump system (Shimadzu, Kyoto, Japan) coupled with a high-pH reverse-phase liquid chromatography column. The labeled peptides were reconstituted with buffer A (5% ACN, 95% H_2O, pH 9.8) to 2 mL and loaded onto a column containing 5-μm particles (Phenomenex, USA). The peptides were separated with a gradient of 5% buffer B (5% H2O, 95% ACN, pH 9.8) at a flow rate of 1 mL/min for 10 min, 5–35% buffer B for 40 min, and 35–95% buffer B for 1 min. The system was then maintained in 95% buffer B for 3 min, and decreased to 5% within 1 min before equilibrating with 5% buffer B for 10 min. The eluate was monitored by absorbance at 214 nm, and fractions were collected every 1 min. All eluted peptides were pooled as 20 fractions and vacuum-dried. Each dried peptide fraction was resuspended in buffer A (2% ACN and 0.1% formic acid in water) and centrifuged at 20,000*g* for 10 min. The supernatant was loaded onto a C18 trap column at a rate of 5 μL/min for 8 min, using an LC-20AD nano-HPLC instrument (Shimadzu, Kyoto, Japan), by the autosampler. Then, peptides were eluted from the trap column and separated by an analytical C18 column (inner diameter 75 μm) packed in-house. The gradient was run at 300 nL/min starting from 8 to 35% of buffer B (2% H_2O and 0.1% formic acid in ACN) over 35 min and going up to 60% in 5 min, then maintained at 80% B for 5 min before returning to 5% in 0.1 min and equilibrating for 10 min. Data acquisition was performed with a Triple TOF 5600 System (SCIEX, USA) equipped with a Nanospray III source (SCIEX, USA), a pulled quartz tip as the emitter (New Objectives, Woburn, MA) and controlled by software Analyst 1.6 (AB SCIEX, Concord, ON). Data was acquired with the following MS conditions: ion spray voltage 2300 V, a curtain gas of 30, nebulizer gas of 15, and interface heater temperature of 150 °C. The high sensitivity mode was used for the entire data acquisition. The accumulation time for MS1 was 250 ms, and the mass ranges were from 350 to 1500 Da. Based on the intensity in the MS1 survey, as many as 30 product ion scans were collected if exceeding a threshold of 120 counts per second (counts/s) and with a charge-state of 2 + to 5 +. Dynamic exclusion was set for 1/2 of the peak width (12 s). For iTRAQ data acquisition, the collision energy was adjusted to all precursor ions for collision-induced dissociation, and the Q2 transmission window for 100 Da was 100%.

2.5. Protein identification and data analysis

The raw MS/MS data was converted into an MGF format by the msConvert tool in ProteoWizard (Oxford, England) (Kessner et al., 2008). Protein identification was performed using the Mascot version 2.3.02 (Matrix Science, London, UK), and searching against the non-redundant National Center for Biotechnology Information database of human protein sequences. Parameters were the following: MS/MS ion search, peptide mass tolerance at 0.05 Da and fragment tolerance was at 0.1 Da, trypsin was the enzyme, variable modifications were defined as oxidation of methionine and iTRAQ 8-plex labeled tyrosine, and carbamidomethyl (C), iTRAQ 8-plex (K) and iTRAQ 8-plex (N-term), as fixed modifications. The peptide-spectra (PSMs) were pre-filtered at a PSM-level false discovery rate (FDR) of 1% to assess the confidence level of the peptides (Savitski et al., 2015). The confident identification of each protein involved at least one unique peptide. For protein quantization, a protein must contain at least two unique peptides. Anautomated software called IQuant was used for quantitatively analyzing the labeled peptides with isobaric tags (Wen et al., 2014). We defined the differentially-expressed proteins to 1.2-fold increased or 0.83-fold decreased expression change in at least one replicate experiment, and ratios with $P < 0.05$ (Zhu et al., 2009). All the proteins with an FDR < 1% were used for downstream analysis, including Gene Ontology (GO) and KEGG pathway analysis. Functional annotations of the proteins were conducted with the GO program against the non-redundant protein database. Further, the GO enrichment terms of differential proteins against the background of identified proteins were identified by the hypergeometric test ($P < 0.05$).

2.6. Enzyme-linked immunosorbent assay (ELISA) analysis

For ELISA analysis, from each of the 300 enrolled subjects, 100 mg umbilical tissue was rinsed with PBS, and then homogenized, in total protein lysis buffer (Bestbio, China), using a Pro200 homogenizer (Pro Scientific, USA). Homogenates were centrifuged for 15 min at 12,000*g*, 4 °C. The supernatant was collected and the concentration of proteins of interest was assayed by ELISA using a kit from Bio-Swamp (China) according to the manufacturer's instructions.

2.7. Statistical analysis

The independent-sample *t*-test or chi-square test was utilized to determine the difference between two groups. Median and range values were used to depict the PBDE levels, which were lipid-adjusted and presented as ng/g lw (lipid weight), lipid-adjusted PBDE concentration was used in the data analysis, and the Mann-Whitney *U* test was used for significant differences. The Σ_{14}PBDEs was defined as the sum of 14 congeners in umbilical cord tissue. As PBDE concentrations were not normally distributed, they were log10 transformed to approximate a normal distribution. PBDE levels below the detection limit were designated as ND (not detectable) and treated as zero for the analysis (Zhao et al., 2013). Spearman's rank correlation analysis was performed to analyze the relationships of the differentially-expressed proteins and neonatal birth outcomes. Multiple linear regression analysis adjusting for confounding factors (e.g. neonatal gender, gestation age, maternal alcohol and passive smoking during pregnancy) was used to model the association between log10-transformed PBDE concentrations and three differentially-expressed proteins in the umbilical cord. A $P < 0.05$ in a two-tailed test was considered as statistically significant. Statistical analyses were conducted using statistical software SPSS version 20.0 (SPSS Inc., Chicago, IL, USA).

3. Results

3.1. Demographic characteristics of the study population

A total of 150 pregnant women from Guiyu and 150 pregnant women from Haojiang were enrolled and provided umbilical cord tissues for this study (Table 1, $P < 0.01$). Compared with the reference group, the gestation age in the e-waste-exposed group was increased ($P < 0.01$). Both body mass index (BMI) of neonates and pregnant women (women prior to pregnancy) shows a significant difference ($P < 0.05$). No significant difference was found in birth weight and neonatal gender between the two groups. The other indices of neonatal

Table 1
Characteristics of the study population in the exposed and reference groups.

Characteristics	Guiyu (n = 150) Mean ± SD	Haojiang (n = 150) Mean ± SD	P-value
Maternal age (years)	26.51 ± 3.86	28.43 ± 4.81	< 0.001[a]
Gestational age (weeks)	39.90 ± 0.78	39.57 ± 1.39	< 0.001[a]
Passive smoking [(n (%)]			0.534[b]
Yes	65 (43.33)	56 (37.33)	
No	85 (56.67)	94 (62.67)	
Maternal alcohol [(n (%)]			0.215[b]
Yes	5 (3.33)	1 (0.67)	
No	145 (96.67)	149 (99.33)	
Neonatal gender [(n (%)]			
Male	87 (58.00)	71 (52.70)	0.065[b]
Female	63 (42.00)	79 (47.30)	
Neonatal body length (cm)	51.40 ± 2.04	50.25 ± 1.00	< 0.001[a]
Neonatal birth weight (g)	3189.67 ± 398.75	3239.67 ± 430.83	0.298[a]
Neonatal head circumference (cm)	32.98 ± 3.17	35.16 ± 1.55	< 0.001 [a]
Neonatal BMI (kg/m^2)	12.07 ± 1.39	12.80 ± 1.47	< 0.001[a]
Pre-pregnant BMI (kg/m^2)	18.61 ± 4.74	20.28 ± 4.41	< 0.001[a]
Neonatal Apgar1 score	9.61 ± 0.54	9.98 ± 0.33	< 0.001[a]
Σ_{14}PBDEs (ng/g lw)[c]	71.92 (8.95–440.08)	15.52 (1.65–182.81)	< 0.001

[a] Analysis using the independent-samples t-test.
[b] Analysis using the chi-square test.
[c] Sum of 14 individual PBDE congeners; median values; Mann-Whitney U test.

growth and development, including head circumference and Apgar1 score, were lower in the exposed group than in the Haojiang group ($P < 0.01$), whereas neonatal body length in the exposed group was higher ($P < 0.01$).

3.2. PBDE levels in umbilical cord

Fourteen PBDE congeners were detected in the umbilical cord. The median umbilical cord concentration of Σ_{14}PBDEs in the exposed group umbilical cord samples (median: 71.92 ng/g lw; range: 8.95–440.08 ng/g lw) was approximately five times higher than in Haojiang (median: 15.52 ng/g lw; range: 1.65–182.81 ng/g lw) (Table 1). The distribution of individual congener concentrations is shown in Table S1.

3.3. Differentially-expressed umbilical cord proteins under PBDE exposure

3.3.1. Protein identification and quantification

We conducted high-throughput iTRAQ labeling proteomic technology to identify the expression changes of umbilical cord tissue proteins associated with PBDE exposure. A total of 3969 non-redundant proteins were identified, with an FDR < 1%. The protein ratio distribution of fold change is shown in Fig. 1. Compared with the reference group, 697 proteins were identified as differentially expressed. Among them, 386 proteins were up-regulated, while 311 proteins were down-regulated (Table S2). Of the 697 differentially-expressed proteins, several proteins were related to antioxidant activity and apoptosis, including catalase (CAT), glutathione S-transferase omega-1 (GSTO1) and cytochrome c (Cyt c) (Table 2).

3.3.2. The classification of identified proteins by functional categories

Based on GO analysis, the identified differentially-expressed proteins were classified into molecular functions (Fig. 2), including antioxidant activity (1.32%), binding (48.59%), catalytic activity (23.02%), enzyme regulator activity (5.11%), channel regulator activity (0.35%), chemoattractant activity (0.18%), electron carrier activity (0.97%), molecular transducer activity (2.65%), nucleic acid-binding transcription factor activity (0.88%), protein-binding transcription factor activity (0.62%), receptor activity (1.85%), receptor regulator activity (0.26%), structural molecule activity (9.79%), and transporter activity (4.41%). Additionally, GO analysis based on biological process showed

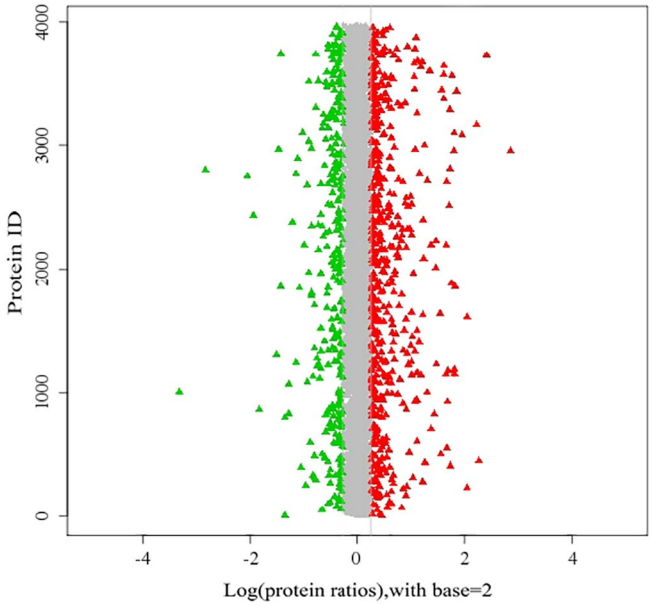

Fig. 1. The protein ratio distribution of differentially-expressed proteins in umbilical cord tissue between the exposed and reference groups. A red dot signifies an up-regulated protein, and a green dot signifies a down-regulated protein. (For interpretation of the references to color in this figure legend, the reader is referred to the web version of this article.)

that the differentially-expressed proteins were principally in association with cellular, metabolic, developmental process and cell killing (Fig. S1). Pathway enrichment based on the KEGG database generated a scatterplot of pathway terms of differentially-expressed proteins (Fig. 3).

3.3.3. ELISA validation

We performed an ELISA assay for 300 umbilical cord samples to verify the differentially-expressed proteins identified by iTRAQ analysis. The expression of CAT and GSTO1 in the exposed groups was lower than the reference umbilical cord tissue samples (902.49 ± 98.42 vs. 1305.13 ± 127.90 pg/g wt, and 525.92 ± 91.08 vs. 561.65 ± 103.81 pg/g wt, $P < 0.01$, respectively). Cyt c expression was higher than in the reference group

Table 2
List of differentially-expressed proteins in umbilical cord tissue from reference and e-waste-exposed groups, including Gi number, protein name, mass, coverage, number of peptides, functional description and variation.

No.	Gi number[b]	Protein name	Mass	Coverage	No. of peptides	Functional description	Variation[a]
Antioxidant activity							
3251	gi|4557014	Catalase	59,928.83	0.476	15	Antioxidant and binding catalytic activity	− 0.70
449	gi|4758484	Glutathione S-transferase omega-1	27,815.13	0.436	10	Antioxidant and catalytic activity	− 0.85
1123	gi|50592994	Thioredoxin isoform 1	11,996.84	0.476	5	Binding catalytic and electron carrier activity	− 0.93
3288	gi|20149576	Nuclear factor erythroid 2-related factor 2	68,108.55	0.015	1	Binding nucleic acid binding transcription factor activity	+ 3.31
1243	gi|4504349	Hemoglobin subunit beta	16,084.32	0.999	8	Antioxidant, binding catalytic and transporter activity	− 0.45
2692	gi|32189392	Peroxiredoxin-2	22,031.29	0.657	9	Antioxidant and catalytic activity	− 0.68
3055	gi|148596959	Redox-regulatory protein FAM213A isoform 1 precursor	25,843.47	0.166	3	antioxidant activity	− 0.78
872	gi|4758638	Peroxiredoxin-6	25,115.22	0.719	12	Antioxidant and binding catalytic activity	− 0.95
3942	gi|46276889	Bone marrow proteoglycan isoform 1 preproprotein	25,855.50	0.315	6	Antioxidant, binding catalytic, receptor regulator and structural molecule activity	− 1.04
78	gi|4502027	Serum albumin preproprotein	71,299.24	0.999	50	Antioxidant activity binding	+ 1.09
1174	gi|4504699	Inhibin beta A chain precursor	48,192.30	0.099	3	Binding	+ 1.21
1354	gi|6006001	Glutathione peroxidase 3 precursor	25,746.98	0.190	4	Antioxidant and binding catalytic activity	+ 1.07
1650	gi|93163358	Apolipoprotein A-IV	45,353.46	0.588	17	Antioxidant and binding enzyme regulator and transporter activity	+ 1.09
2931	gi|22091452	Apolipoprotein M isoform 1	21,563.56	0.176	2	Antioxidant and binding transporter activity	+ 1.23
3417	gi|4557325	Apolipoprotein E precursor	36,227.79	0.309	8	Antioxidant, binding enzyme regulator and transporter activity	+ 1.08
3501	gi|5453549	Peroxiredoxin-4 precursor	30,730.89	0.306	5	Antioxidant and binding catalytic activity	+ 1.08
3803	gi|109150416	Peroxidasin homolog precursor	167,774.85	0.195	15	Antioxidant, binding catalytic, receptor regulator and structural molecule activity	+ 1.11
Apoptosis							
1091	gi|11128019	Cytochrome c	11,837.16	0.724	6	Binding catalytic and electron carrier activity	+ 1.05
298	gi|317373596	Calpain-2 catalytic subunit	80,782.10	0.376	16	Binding catalytic activity	− 0.99
437	gi|12,408,656	Calpain-1 catalytic subunit	82,447.41	0.371	17	Binding catalytic activity	− 0.90
1012	gi|115298659	Spectrin alpha chain, erythrocytic 1	281,021.34	0.048	5	Binding structural molecule activity	− 0.78
1359	gi|6678467	Tubulin alpha-4A chain	50,615.64	0.580	2	Binding catalytic and structural molecule activity	− 0.94
1526	gi|154759259	Spectrin alpha chain, non-erythrocytic 1 isoform 2	285,144.50	0.328	43	Binding structural molecule activity	− 0.95
663	gi|11545918	Tubulointerstitial nephritis antigen-like isoform 1 precursor	53,703.46	0.385	9	Binding catalytic, receptor, and structural molecule activity	+ 1.17
1086	gi|5579478	Dual specificity mitogen-activated protein kinase kinase 1	43,735.40	0.229	6	Binding catalytic, enzyme regulator and molecular transducer activity	+ 1.27
3039	gi|91718899	Mitogen-activated protein kinase 3 isoform	43,432.23	0.214	3	Binding catalytic and molecular transducer activity	+ 1.21

[a] Compared with the reference group, the mean ratio of three replicates. The differentially-expressed proteins change at least in one replicate experiment above 1.2-fold and below 0.83-fold change, indicated by + and −, respectively, $P < 0.05$.
[b] From the NCBInr database.

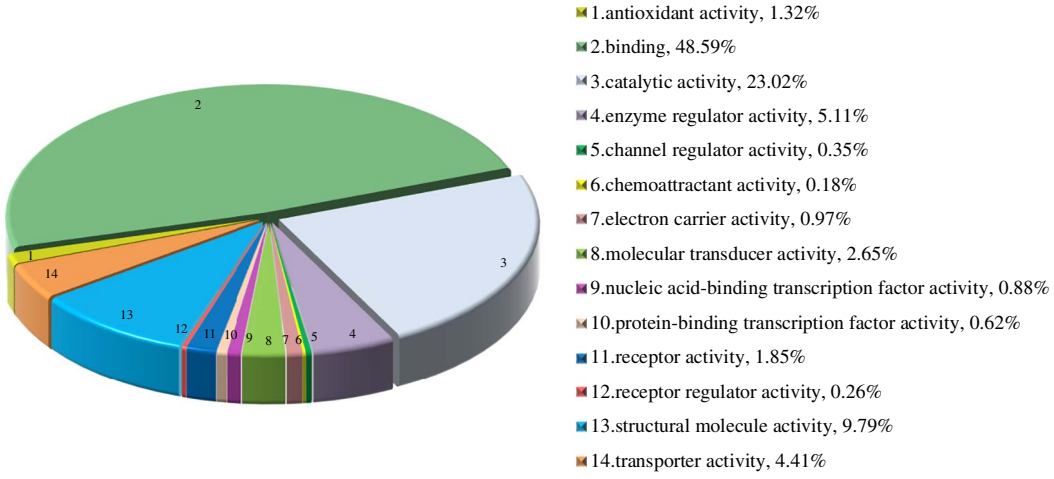

Fig. 2. Classification of the identified differentially-expressed proteins into molecular functions.

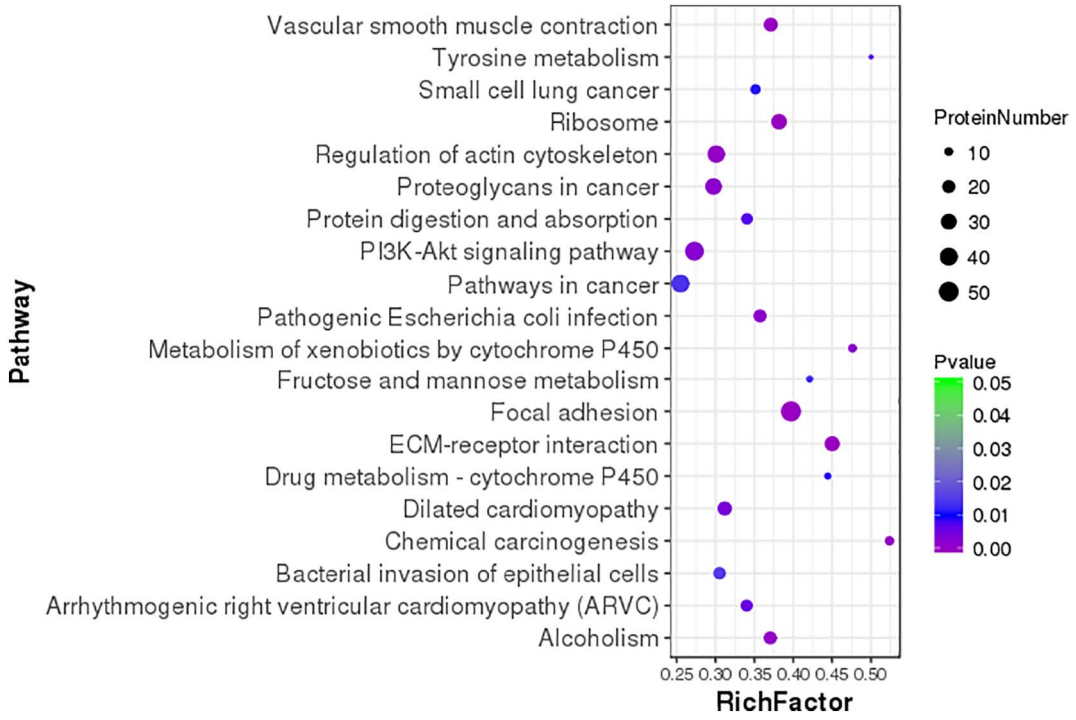

Fig. 3. The KEGG pathway enrichment of differentially-expressed proteins. Rich factor and *P*-value indicate the intensiveness of enrichment. The scale of plots stands the protein number.

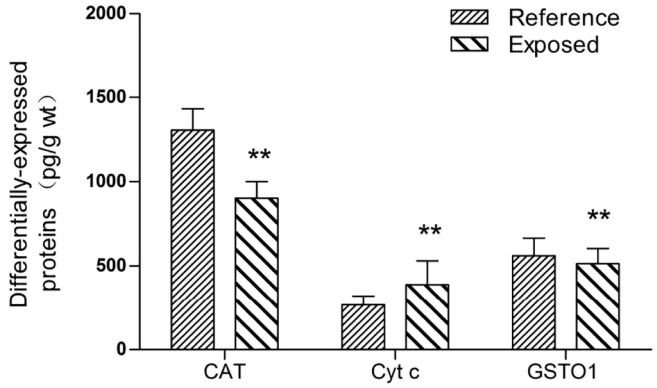

Fig. 4. ELISA analysis of catalase (CAT), glutathione S-transferase omega-1 (GSTO1) and cytochrome c (Cyt c) of umbilical cord tissue from exposed group and reference group. ** Significant at $P < 0.01$.

(389.37 ± 141.34 vs. 267.98 ± 52.06 pg/g wt, $P < 0.01$). As shown in Fig. 4, the ELISA results were essentially consistent with the iTRAQ results.

3.4. Associations between PBDE levels in umbilical cord tissue and biological endpoints

Spearman's correlation test revealed a positive correlation between neonatal BMI and Apgar1 score, neonatal BMI and head circumference, neonatal body length and Apgar1 score, head circumference and Apgar1 score ($P < 0.01$) (Table 3). The Σ_{14}PBDEs was negatively correlated with neonatal BMI, Apgar1 score, neonatal body length and head circumference ($P < 0.01$). For CAT and GSTO1, higher levels of total PBDE exposure were associated with decreased CAT and GSTO1 ($P < 0.01$). For Cyt c, elevated concentrations of total PBDE were significantly associated with increased Cyt c ($P < 0.01$). The expression of CAT was positively associated with neonatal BMI, neonatal Apgar1 score and neonatal head circumference, but negatively associated with neonatal body length ($P < 0.01$). There were negative correlations between GSTO1 and neonatal body length ($P < 0.05$). Cyt c was negatively related to neonatal Apgar1 score ($P < 0.01$), and positively related to neonatal body length ($P < 0.01$). While no significant association was found between GSTO1 and neonatal BMI, Cyt c and neonatal BMI. A positive correlation was observed between CAT and Cyt c, GSTO1 and Cyt c ($P < 0.01$), and a negative correlation was observed between CAT and GSTO1 ($P < 0.01$).

Multiple linear regression models were conducted to model the

Table 3
Spearman's correlation between PBDE levels in umbilical cord and biological endpoints.

Variables	Neonatal BMI	Apgar1score	Neonatal body length	Head circumference	CAT	GSTO1	Cyt c
Neonatal BMI	1	–	–	–	–	–	–
Apgar1 score	0.243**	1	–	–	–	–	–
Neonatal body length	− 0.049	− 0.289**	1	–	–	–	–
Head circumference	0.450**	0.234**	0.069	1	–	–	–
CAT	0.215**	0.386**	− 0.329**	0.294**	1	–	–
GSTO1	− 0.050	0.056	− 0.136*	− 0.031	0.449**	1	–
Cyt c	− 0.013	− 0.165**	0.221**	− 0.074	− 0.590**	− 0.956**	1
Σ_{14}PBDEs	− 0.196**	− 0.395**	0.346**	− 0.375**	− 0.714**	− 0.172**	0.369**

* $P < 0.05$.
** $P < 0.01$.

Table 4
Multiple linear regression analysis[a] for associations between PBDE concentrations and three differentially-expressed proteins in umbilical cord.

	CAT	GSTO1	Cyt c
	β (95% CI)	β (95% CI)	β (95% CI)
BDE-17	− 0.097 (− 0.047, − 0.004)*	− 0.100 (− 0.005, 0.050)	− 0.050 (− 0.066, 0.025)
BDE-28	0.069 (− 0.006, 0.035)	0.062 (− 0.015, 0.038)	− 0.048 (− 0.060, 0.028)
BDE-47	− 0.017 (− 0.019, 0.013)	− 0.038 (− 0.026, 0.015)	0.059 (− 0.019, 0.048)
BDE-66	0.033 (− 0.017, 0.029)	0.143 (− 0.006, 0.053)	− 0.163 (− 0.097, 0.000)*
BDE-71	− 0.084 (− 0.032, 0.003)	− 0.007 (− 0.024, 0.021)	− 0.044 (− 0.025, 0.048)
BDE-85	0.012 (− 0.019, 0.023)	0.068 (− 0.015, 0.039)	− 0.091 (− 0.073, 0.016)
BDE-99	− 0.160 (− 0.050, − 0.012)**	− 0.142 (− 0.048, 0.001)	0.165 (0.009, 0.089)*
BDE-100	0.031 (− 0.014, 0.026)	0.010 (− 0.024, 0.027)	0.072 (− 0.021, 0.063)
BDE-138	− 0.062 (− 0.034, 0.009)	− 0.068 (− 0.039, 0.016)	− 0.062 (− 0.034, 0.009)
BDE-153	0.020 (− 0.024, 0.032)	− 0.202 (− 0.072, − 0.001)*	0.175 (− 0.002, 0.115)
BDE-154	0.026 (− 0.015, 0.024)	0.064 (− 0.016, 0.035)	− 0.079 (− 0.063, 0.021)
BDE-183	− 0.195 (− 0.056, − 0.013)**	− 0.061 (− 0.037, 0.018)	0.078 (− 0.024, 0.061)
BDE-190	− 0.013 (− 0.019, 0.015)	− 0.163 (− 0.045, − 0.002)*	0.189 (0.013, 0.084)**
BDE-209	− 0.168 (− 0.066, 0.002)	0.065 (− 0.033, 0.055)	− 0.092 (− 0.099, 0.045)
Σ_{14}PBDEs	− 0.315 (− 0.155, − 0.001)*	− 0.054 (− 0.111, 0.088)	0.228 (− 0.075, 0.251)

* $P < 0.05$.
** $P < 0.01$.
[a] Adjusted for neonatal gender, gestation age, maternal alcohol and passive smoking during pregnancy.

associations between PBDE exposure and three differentially-expressed proteins in umbilical cord (Table 4). For CAT, a log-unit increase in levels of BDE-17, BDE-99, BDE-183, BDE-209 and Σ_{14}PBDEs was associated with a 0.10% (β = − 0.097; 95% CI, − 0.047 to − 0.004), 0.16% (β = − 0.160; 95% CI, − 0.050 to − 0.012), 0.20% (β = − 0.195; 95% CI, − 0.056 to − 0.013) and 0.32% (β = − 0.315; 95% CI, − 0.155 to − 0.001) decrease in CAT expression in umbilical cord tissue, respectively. The GSTO1 expression was found to significantly decrease with a log-unit increase of BDE-153 (β = − 0.202; 95% CI, − 0.072 to − 0.001) and BDE-190 (β = − 0.163; 95% CI, − 0.045 to − 0.002). For Cyt c, a log-unit increase in umbilical cord concentration of BDE-66 was associated with a 0.16% (β = − 0.163; 95% CI, − 0.097 to − 0.000) decrease in Cyt c expression. However, increases in BDE-99 and 190 were associated with 0.17% (β = 0.165; 95% CI, 0.009 to 0.089) and 0.19% (β = 0.189; 95% CI, 0.013 to 0.084) increases in Cyt c expression, respectively.

4. Discussion

In this study, we characterized the protein profile changes and PBDE burden in umbilical cords from Guiyu and Haojiang, China. The high PBDE exposure levels in the exposed group are consistent with our previous study on PBDE concentrations in placenta tissues and umbilical cord blood (Wu et al., 2010; Xu et al., 2015). We found the distance of residence from an e-waste recycling workshop mostly contributes to PBDE concentrations in umbilical cord tissue samples. Although a great deal of studies, to date, have been demonstrated the association between PBDE levels in umbilical cord or placenta and neonatal health, there are no studies investigating whether PBDE levels in umbilical cord are associated with fetal development and growth. The umbilical cord plays an important role in the transport of nutrients and oxygen between fetus and mother (Kawashiro et al., 2009). This is the first study to gain differentially-expressed proteins in e-waste-exposed umbilical cord tissues. For proteomic analysis, we identify 697 differentially-expressed proteins, which are mainly involved in antioxidant defense, apoptosis, cell structure and metabolism. Moreover, the pathway enrichment analysis shows many differentially-expressed proteins are involved in the chemical carcinogenesis pathway. This indicates that PBDE exposure might pose potential carcinogenic risk (Song et al., 2009).

Previous studies show that PBDEs could disrupt cellular redox balance and induce oxidative stress by triggering excessive production of reactive oxygen species (ROS), leading the oxidation of proteins, nucleic acids and lipids, and contributing to cell apoptosis (Nordberg and Arner, 2001; Silva et al., 2016). Nonetheless, ROS can be removed by the antioxidant defense system consisting of cellular antioxidant enzymes (Suzuki et al., 2012). CAT, an antioxidant enzyme, protects cells against ROS-induced oxidative damage by catalyzing the decomposition of hydrogen peroxide to water and oxygen (Chelikani et al., 2004). Previous studies found BDE-47 and BDE-209 exposure could induce CAT expression and activate the enzyme activity (Farzana et al., 2016; He et al., 2008). However, in this study, CAT was identified as a down-regulated protein in umbilical cord tissue in response to PBDE stress. Interestingly, this difference is in agreement with a prior study that found BDE-209 significantly inhibits CAT gene expression induced by lead in the earthworm (Zhang et al., 2015). The possible reason for PBDE-induced CAT downregulation might be associated with excessive generation of ROS following long-term PBDE exposure, resulting in DNA oxidative damage (Ji et al., 2011). The transcriptional expression of antioxidant enzyme genes is stimulated to prevent the replication of damaged cells, a model strongly supported by Kono and Fridovich (1982), who reported that stress conditions possibly generated excess O^{2-}, which leads to the inhibition of CAT activity.

Another antioxidant enzyme in the glutathione antioxidant system is GSTO1, which is also decreased in the e-waste-exposed group in our study. Similarly, Wang et al. (2015) indicated that the activities of glutathione transferases (GSTs) negatively correlated with BDE-47 concentration. GSTO1, a GST superfamily member, catalyzes glutathione conjugation with electrophiles and reduces oxidative stress by conjugating the end-products of lipid peroxides to glutathione (Reinemer et al., 1992; Strange et al., 2001). The activities of GSTs also are regulated by over producing ROS under PBDE exposure, leading to decreased oxidation resistance and the toxic effect of GST (Zhao et al., 2011). In our study, the positive correlation between CAT and GSTO1 suggests that PBDE exposure negatively affects antioxidant capacity by decreasing CAT and GSTO1 expression. Additionally, other antioxidants, including thioredoxin, glutathione peroxidase, peroxiredoxins, apolipoprotein, and peroxidasin, also are regulated in umbilical cords. Thioredoxin (Trx) is an antioxidant and encoded by the *TXN* and *TXN2* genes, which have been found to have altered expression in human umbilical vein endothelial cells following PBDE exposure (Kawashiro et al., 2009). Similarly, we find that thioredoxin is down-regulated in umbilical cord tissue in the Guiyu group. Glutathione peroxidase plays an important role in maintaining the antioxidant balance, and its activity is influenced by BDE-47 (Barranco-Medina et al., 2009; Hossain and Komatsu, 2012; Wang et al., 2015).

Peroxiredoxin, a thiol peroxidase, detoxifies hydroperoxides, and plays a vital role in enzyme activation and redox sensing. A prior study observed that expression levels of peroxiredoxin are up-regulated under heavy metal stress conditions. Moreover, the nuclear transcription factor (erythroid-derived 2)-like 2 (Nrf2) is down-regulated in this study. Nrf2 plays an important role in environmental toxicant exposure-induced signal pathway responses, and regulates the expression of antioxidant proteins that protect against oxidative damage (Gold et al., 2012; Hybertson et al., 2011; Kodavanti et al., 2015). Under oxidative stress, Nrf2 travels to nucleus and actives transcription of antioxidative genes and proteins, including NAD(P)H quinone oxidoreductase 1, GST and thioredoxin (Kweider et al., 2014). Therefore, the alteration of the above-mentioned proteins CAT, GSTO1, Trx, PRDX2, PRDX6, and Nrf2 may contribute to an imbalance between oxidation and antioxidation, leading to a lack of protection against ROS-induced oxidative stress upon PBDE exposure. Thus, excess endogenous ROS could be released, leading to severe oxidative damage, and causing cell physiological disorders in the umbilical cord, which in turn may affect fetal development and growth and the medical value of stem cells.

An increasing number of studies indicate that PBDE exposure also causes apoptosis in neurons (Zhang et al., 2013). Cyt c is a component of the electron transport chain in the inner mitochondrial membrane and released into cytoplasm to initiate apoptosis. Mitochondrial Cyt c release could be facilitated by disruption of mitochondrial membrane potential under ROS stress (Munoz-Pinedo, 2012; Souza et al., 2013). It is reported that BDE-47 exposure can cause neurotoxic effects by inducing human neuroblastoma SH-SY5Y cell apoptosis via the tumor suppressor p53-dependent mitochondrial apoptotic pathway (Zhang et al., 2013). The author found the apoptotic pathway mainly involved up-regulation of p53 and pro-apoptotic protein BAX, downregulation of anti-apoptotic protein Bcl-2 and Bcl-2/Bax ratio, and caspase-9 apoptosis pathway. In the present study, Cyt c is up-regulated under PBDE exposure in umbilical cord tissue. This is in line with the report of Yu et al., who demonstrated that Cyt c release and caspase-3 activation are observed in SK-N-SH cells (human neuroblastoma cells) treated with BDE-71 (12.8 and 25.6 μmol/L) (Yu et al., 2008). A negative correlation between CAT and Cyt c, GSTO1 and Cyt c was found in this study, signaling disruption of the antioxidant system might contribute to the Cyt c-mediated cell apoptosis. Furthermore, other proteins related to the apoptosis pathway, such as mitogen-activated protein kinase 3 (MAPK3), dual specificity mitogen-activated protein kinase kinase (MAP2K1) and calpain catalytic subunit (CAPN1, CAPN2), have also been found to be abnormally expressed in this study. MAPK3 is a member of mitogen-activated protein kinase (MAPK) family, and is involved in a signaling cascade that regulates cell apoptosis (Cao et al., 2017; Pearson et al., 2001). Xu et al. (2016b) found that p38 MAPK-related signal transduction pathways are dramatically activated by ROS generation following cadmium treatment associated with induction of apoptosis in human bronchial epithelial cells. MAP2K is a kinase enzyme that phosphorylates MAPK and interacts with MAPK3 (Zheng and Guan, 1993). Calpain, a protein belonging to the family of calcium-dependent proteases, has been implicated in apoptotic cell death (Nimmrich et al., 2010). CAPN2 has been shown to interact with Bcl-2 to decrease of Bcl-2 protein, provoking Cyt c release from mitochondria, thereby triggering the intrinsic apoptotic pathway (Gil-Parrado et al., 2002). In this study, the dysfunction of Cyt c and other apoptosis-related proteins show that the apoptosis pathway in the umbilical cord may be activated by PBDE exposure.

Additionally, in the present study, pathway enrichment analysis shows significant enrichment of pathways involved in chemical carcinogenesis and signaling pathway. It is reported that oxidative stress is associated with carcinogenesis, excess generation of reactive oxygen can cause DNA damage and modifications (Toyokuni, 2006). The carcinogenic effects of ROS accumulation involve changes in gene expression, increase proliferation and DNA mutational rates, and genomic instability (Allen and Tresini, 2000; Dolado et al., 2007; Woo and Poon, 2004). Especially, mitochondrial DNA (mtDNA), an important target of endogenous ROS in the context of cancer initiation, as mutations in mtDNA seem to be capable of promoting tumorigenesis (Sabharwal and Schumacker, 2014). Mitochondrial oxidants also contribute to genomic instability (Ishikawa et al., 2008). However, the mechanism of PBDE-induced carcinogenesis was complicated and still unclear. PI3K-Akt pathway, a well-known apoptosis-relevant signaling. Previously, the literature has reported that the PI3K-Akt signaling pathway was involved in apoptosis by releasing Cyt c into the cytoplasm, and the mitochondrial apoptosis pathway (Sui et al., 2015). Thus the effects of PBDE by chemical carcinogenesis and signaling pathway may relate to cell oxidative stress and apoptosis, and we need more evidences in the future work.

In this study, we conducted proteomic analysis in the umbilical cord, following PBDE exposure, and identified biomarkers, such as CAT and GSTO1, which are involved in protection against cell oxidative damage, and Cyt c, which is in involved cell apoptosis. Moreover, toxic effects also involved in cell structure, metabolism and even carcinogenesis, and could enhance the knowledge in understanding the effects observed following exposure to PBDEs. Collectively, the differentially-expressed proteins are associated with protection against oxidative stress under PBDE exposure. Long-term oxidative stress could trigger cell oxidative damage, including membrane lipid peroxidation, oxidative modification of proteins, DNA damage and mutation. Mitochondrial injury induced by oxidative stress could trigger mitochondrial endogenous ROS production and release of cytochrome c into the cytoplasm, resulting in cell oxidative damage enlarging and even apoptosis. In our study, CAT and GSTO1 are negatively related to Cyt c, which could contribute to the cell apoptosis. Moreover, decreased expression of antioxidant enzymes under PBDE exposure prevents cells from being protected against excessive ROS. Thus, antioxidant imbalance plays a critical role in initial cell process. Moreover, we investigated the relationship between PBDE levels in umbilical cord and fetal growth and development, and found that the PBDE concentrations in umbilical cord are negatively related to neonatal BMI, consistent with our prior study showing neonatal BMI is inversely associated with placenta PBDE levels (Xu et al., 2015). Additionally, PBDE levels negatively correlated with neonatal head circumference and Apgar1 score. However, there is no statistically significant association found between umbilical PBDE levels and neonatal gender, gestational age and birth weight. This could be due to exposure dose and duration, different tissues or organs in neonatal growth and co-exposure conditions. Altered gene expressions of the antioxidant system may affect fetal development and growth (Kawashiro et al., 2009). Our data of the association between umbilical PBDE exposure and neonatal birth outcomes suggest that the alterations in umbilical cord antioxidant proteins, such as CAT and GSTO1, could be responsible for alterations in neonatal parameters. For instance, the expression of CAT and GSTO1 in umbilical cord is negatively associated with neonatal body length, CAT expression is positively associated with neonatal BMI and Apgar1, and Cyt c positively associated with neonatal body length, suggesting that CAT, GSTO1 and Cyt c may directly or indirectly affect neonatal early growth and development. Further study is needed to confirm the health risk evaluation in the future.

5. Conclusion

This is the first study applying iTRAQ-based proteomic analysis to show an association between in utero PBDE exposure and neonatal birth outcomes in human umbilical cord from e-waste area. However, there are some limitations due to the lack of sufficient specimens to identify more contaminants resulting from a complicated e-waste exposure environment in Guiyu. Hence, the combination of co-exposure and its potentially interactive effects should be given attention in the next step of the study. Additionally, umbilical cord tissue contains multifarious cell types. Further study is needed to investigate the

differentially-expressed proteins targets in specific cell types. In this study, we only conducted ELISA validation on enzyme expression rather than activity. For proteomic analysis, we only reported the effects of PBDE exposure on three candidate proteins. Other altered proteins and their interaction networks should be investigated in the future work.

Supplementary data to this article can be found online at https://doi.org/10.1016/j.envint.2017.09.016.

Acknowledgments

The work was supported by the National Natural Science Foundation of China [grant numbers 21577084]; The Natural Science Foundation of Guangdong Province [grant numbers 2015A030313435]; and Education Department of Guangdong Government Development Scheme for Research and Control of Infectious Diseases [grant numbers 2015082]. We would like to thank Dr. Stanley Lin for his constructive comments and English language editing. We are grateful to all the recruited puerperants for participating in this project.

References

Abdallah, M.A., Harrad, S., 2014. Polybrominated diphenyl ethers in UK human milk: implications for infant exposure and relationship to external exposure. Environ. Int. 63, 130–136.
Allen, R.G., Tresini, M., 2000. Oxidative stress and gene regulation. Free Radic. Biol. Med. 28, 463–499.
Alm, H., Scholz, B., Fischer, C., Kultima, K., Viberg, H., Eriksson, P., Dencker, L., Stigson, M., 2006. Proteomic evaluation of neonatal exposure to 2,2,4,4,5-pentabromodiphenyl ether. Environ. Health Perspect. 114, 254–259.
Barranco-Medina, S., Lazaro, J.J., Dietz, K.J., 2009. The oligomeric conformation of peroxiredoxins links redox state to function. FEBS Lett. 583, 1809–1816.
Bradley, B.P., Shrader, E.A., Kimmel, D.G., Meiller, J.C., 2002. Protein expression signatures: an application of proteomics. Mar. Environ. Res. 54, 373–377.
Cao, C., Su, Y., Han, D., Gao, Y., Zhang, M., Chen, H., Xu, A., 2017. Ginkgo biloba exocarp extracts induces apoptosis in Lewis lung cancer cells involving MAPK signaling pathways. J. Ethnopharmacol. 198, 379–388.
Charnley, G., Putzrath, R.M., 2001. Children's health, susceptibility, and regulatory approaches to reducing risks from chemical carcinogens. Environ. Health Perspect. 109, 187–192.
Chelikani, P., Fita, I., Loewen, P.C., 2004. Diversity of structures and properties among catalases. Cell. Mol. Life Sci. 61, 192–208.
Chen, A.K., Reuveny, S., Oh, S.K., 2013. Application of human mesenchymal and pluripotent stem cell microcarrier cultures in cellular therapy: achievements and future direction. Biotechnol. Adv. 31, 1032–1046.
Chen, Z.J., Liu, H.Y., Cheng, Z., Man, Y.B., Zhang, K.S., Wei, W., Du, J., Wong, M.H., Wang, H.S., 2014. Polybrominated diphenyl ethers (PBDEs) in human samples of mother-newborn pairs in South China and their placental transfer characteristics. Environ. Int. 73, 77–84.
Darnerud, P.O., Eriksen, G.S., Johannesson, T., Larsen, P.B., Viluksela, M., 2001. Polybrominated diphenyl ethers: occurrence, dietary exposure, and toxicology. Environ. Health Perspect. 109 (Suppl. 1), 49–68.
Dolado, I., Swat, A., Ajenjo, N., De Vita, G., Cuadrado, A., Nebreda, A.R., 2007. p38alpha MAP kinase as a sensor of reactive oxygen species in tumorigenesis. Cancer Cell 11, 191–205.
Eskenazi, B., Chevrier, J., Rauch, S.A., Kogut, K., Harley, K.G., Johnson, C., Trujillo, C., Sjodin, A., Bradman, A., 2013. In utero and childhood polybrominated diphenyl ether (PBDE) exposures and neurodevelopment in the CHAMACOS study. Environ. Health Perspect. 121, 257–262.
Farzana, S., Chen, J., Pan, Y., Wong, Y.S., Tam, N.F., 2016. Antioxidative response of Kandelia obovata, a true mangrove species, to polybrominated diphenyl ethers (BDE-99 and BDE-209) during germination and early growth. Mar. Pollut. http://dx.doi.org/10.1016/j.marpolbul.2016.12.041.
Gil-Parrado, S., Fernandez-Montalvan, A., Assfalg-Machleidt, I., Popp, O., Bestvater, F., Holloschi, A., Knoch, T.A., Auerswald, E.A., Welsh, K., Reed, J.C., Fritz, H., Fuentes-Prior, P., Spiess, E., Salvesen, G.S., Machleidt, W., 2002. Ionomycin-activated calpain triggers apoptosis. A probable role for Bcl-2 family members. J. Biol. Chem. 277, 27217–27226.
Gold, R., Kappos, L., Arnold, D.L., Bar-Or, A., Giovannoni, G., Selmaj, K., Tornatore, C., Sweetser, M.T., Yang, M., Sheikh, S.I., Dawson, K.T., 2012. Placebo-controlled phase 3 study of oral BG-12 for relapsing multiple sclerosis. N. Engl. J. Med. 367, 1098–1107.
He, P., He, W., Wang, A., Xia, T., Xu, B., Zhang, M., Chen, X., 2008. PBDE-47-induced oxidative stress, DNA damage and apoptosis in primary cultured rat hippocampal neurons. Neurotoxicology 29, 124–129.
Heacock, M., Kelly, C.B., Asante, K.A., Birnbaum, L.S., Bergman, A.L., Bruné, M.N., Buka, I., Carpenter, D.O., Chen, A., Huo, X., Kamel, M., Landrigan, P.J., Magalini, F., Diaz-Barriga, F., Neira, M., Omar, M., Pascale, A., Ruchirawat, M., Sly, L., Sly, P.D., Van den Berg, M., Suk, W.A., 2016. E-waste and harm to vulnerable populations: a growing global problem. Environ. Health Perspect. 124, 550–555.
Hossain, Z., Komatsu, S., 2012. Contribution of proteomic studies towards understanding plant heavy metal stress response. Front. Plant Sci. 3, 310.
Huo, X., Peng, L., Xu, X., Zheng, L., Qiu, B., Qi, Z., Zhang, B., Han, D., Piao, Z., 2007. Elevated blood lead levels of children in Guiyu, an electronic waste recycling town in China. Environ. Health Perspect. 115, 1113–1117.
Hybertson, B.M., Gao, B., Bose, S.K., McCord, J.M., 2011. Oxidative stress in health and disease: the therapeutic potential of Nrf2 activation. Mol. Asp. Med. 32, 234–246.
Ishikawa, K., Takenaga, K., Akimoto, M., Koshikawa, N., Yamaguchi, A., Imanishi, H., Nakada, K., Honma, Y., Hayashi, J., 2008. ROS-generating mitochondrial DNA mutations can regulate tumor cell metastasis. Science 320, 661–664.
Ji, K., Choi, K., Giesy, J.P., Musarrat, J., Takeda, S., 2011. Genotoxicity of several polybrominated diphenyl ethers (PBDEs) and hydroxylated PBDEs, and their mechanisms of toxicity. Environ. Sci. Technol. 45, 5003–5008.
Ji, C., Wu, H., Wei, L., Zhao, J., Yu, J., 2013. Proteomic and metabolomic analysis reveal gender-specific responses of mussel *Mytilus galloprovincialis* to 2,2′,4,4′-tetrabromodiphenyl ether (BDE 47). Aquat. Toxicol. 140-141, 449–457.
Kawashiro, Y., Fukata, H., Omori-Inoue, M., Kubonoya, K., Jotaki, T., Takigami, H., Sakai, S., Mori, C., 2008. Perinatal exposure to brominated flame retardants and polychlorinated biphenyls in Japan. Endocr. J. 55, 1071–1084.
Kawashiro, Y., Fukata, H., Sato, K., Aburatani, H., Takigami, H., Mori, C., 2009. Polybrominated diphenyl ethers cause oxidative stress in human umbilical vein endothelial cells. Hum. Exp. Toxicol. 28, 703–713.
Kessner, D., Chambers, M., Burke, R., Agus, D., Mallick, P., 2008. ProteoWizard: open source software for rapid proteomics tools development. Bioinformatics 24, 2534–2536.
Kodavanti, P.R., Royland, J.E., Osorio, C., Winnik, W.M., Ortiz, P., Lei, L., Ramabhadran, R., Alzate, O., 2015. Developmental exposure to a commercial PBDE mixture: effects on protein networks in the cerebellum and hippocampus of rats. Environ. Health Perspect. 123, 428–436.
Kono, Y., Fridovich, I., 1982. Superoxide radical inhibits catalase. J. Biol. Chem. 257, 5751–5754.
Kweider, N., Huppertz, B., Kadyrov, M., Rath, W., Pufe, T., Wruck, C.J., 2014. A possible protective role of Nrf2 in preeclampsia. Ann. Anat. 196, 268–277.
Leung, A.O., Luksemburg, W.J., Wong, A.S., Wong, M.H., 2007. Spatial distribution of polybrominated diphenyl ethers and polychlorinated dibenzo-p-dioxins and dibenzofurans in soil and combusted residue at Guiyu, an electronic waste recycling site in southeast China. Environ. Sci. Technol. 41, 2730–2737.
Ma, S., Yu, Z., Zhang, X., Ren, G., Peng, P., Sheng, G., Fu, J., 2012. Levels and congener profiles of polybrominated diphenyl ethers (PBDEs) in breast milk from Shanghai: implication for exposure route of higher brominated BDEs. Environ. Int. 42, 72–77.
Martyniuk, C.J., Alvarez, S., Denslow, N.D., 2012. DIGE and iTRAQ as biomarker discovery tools in aquatic toxicology. Ecotoxicol. Environ. Saf. 76, 3–10.
McDonald, T.A., 2002. A perspective on the potential health risks of PBDEs. Chemosphere 46, 745–755.
Miller, M.F., Chernyak, S.M., Batterman, S., Loch-Caruso, R., 2009. Polybrominated diphenyl ethers in human gestational membranes from women in southeast Michigan. Environ. Sci. Technol. 43, 3042–3046.
Munoz-Pinedo, C., 2012. Signaling pathways that regulate life and cell death: evolution of apoptosis in the context of self-defense. Adv. Exp. Med. Biol. 738, 124–143.
Nimmrich, V., Reymann, K.G., Strassburger, M., Schoder, U.H., Gross, G., Hahn, A., Schoemaker, H., Wicke, K., Moller, A., 2010. Inhibition of calpain prevents NMDA-induced cell death and beta-amyloid-induced synaptic dysfunction in hippocampal slice cultures. Br. J. Pharmacol. 159, 1523–1531.
Nordberg, J., Arner, E.S., 2001. Reactive oxygen species, antioxidants, and the mammalian thioredoxin system. Free Radic. Biol. Med. 31, 1287–1312.
Ogunseitan, O.A., Schoenung, J.M., Saphores, J.D., Shapiro, A.A., 2009. Science and regulation. The electronics revolution: from e-wonderland to e-wasteland. Science 326, 670–671.
Pearson, G., Robinson, F., Beers Gibson, T., Xu, B.E., Karandikar, M., Berman, K., Cobb, M.H., 2001. Mitogen-activated protein (MAP) kinase pathways: regulation and physiological functions. Endocr. Rev. 22, 153–183.
Reinemer, P., Dirr, H.W., Ladenstein, R., Huber, R., Lo Bello, M., Federici, G., Parker, M.W., 1992. Three-dimensional structure of class pi glutathione S-transferase from human placenta in complex with S-hexylglutathione at 2.8 A resolution. J. Mol. Biol. 227, 214–226.
Ross, P.L., Huang, Y.N., Marchese, J.N., Williamson, B., Parker, K., Hattan, S., Khainovski, N., Pillai, S., Dey, S., Daniels, S., Purkayastha, S., Juhasz, P., Martin, S., Bartlet-Jones, M., He, F., Jacobson, A., Pappin, D.J., 2004. Multiplexed protein quantitation in *Saccharomyces cerevisiae* using amine-reactive isobaric tagging reagents. Mol. Cell. Proteomics 3, 1154–1169.
Sabharwal, S.S., Schumacker, P.T., 2014. Mitochondrial ROS in cancer: initiators, amplifiers or an Achilles' heel? Nat. Rev. Cancer 14, 709–721.
Savitski, M.M., Wilhelm, M., Hahne, H., Kuster, B., Bantscheff, M., 2015. A scalable approach for protein false discovery rate estimation in large proteomic data sets. Mol. Cell. Proteomics 14, 2394–2404.
Silva, F.S., Simoes, R.F., Couto, R., Oliveira, P.J., 2016. Targeting mitochondria in cardiovascular diseases. Curr. Pharm. Des. 22, 5698–5717.
Sjodin, A., Patterson Jr., D.G., Bergman, A., 2003. A review on human exposure to brominated flame retardants—particularly polybrominated diphenyl ethers. Environ. Int. 29, 829–839.
Solomon, G.M., Weiss, P.M., 2002. Chemical contaminants in breast milk: time trends and regional variability. Environ. Health Perspect. 110, A339–347.
Song, R., Duarte, T.L., Almeida, G.M., Farmer, P.B., Cooke, M.S., Zhang, W., Sheng, G., Fu, J., Jones, G.D., 2009. Cytotoxicity and gene expression profiling of two

hydroxylated polybrominated diphenyl ethers in human H295R adrenocortical carcinoma cells. Toxicol. Lett. 185, 23–31.
Song, J., Li, Z.H., He, Y.T., Liu, C.X., Sun, B., Zhang, C.F., Zeng, J., Du, P.L., Zhang, H.L., Yu, Y.H., Chen, D.J., 2014. Decabrominated diphenyl ether (BDE-209) and/or BDE-47 exposure alters protein expression in purified neural stem/progenitor cells determined by proteomics analysis. Int. J. Dev. Neurosci. 33, 8–14.
Souza, A.O., Pereira, L.C., Oliveira, D.P., Dorta, D.J., 2013. BDE-99 congener induces cell death by apoptosis of human hepatoblastoma cell line - HepG2. Toxicol. in Vitro 27, 580–587.
Strange, R.C., Spiteri, M.A., Ramachandran, S., Fryer, A.A., 2001. Glutathione-S-transferase family of enzymes. Mutat. Res. 482, 21–26.
Sui, Y., Zheng, X., Zhao, D., 2015. Rab31 promoted hepatocellular carcinoma (HCC) progression via inhibition of cell apoptosis induced by PI3K/AKT/Bcl-2/BAX pathway. Tumour Biol. 36, 8661–8670.
Sun, X., Xie, Y., Wu, L., Zhu, W., Hu, J., Lu, R., Xu, W., 2012. Lead acetate reduces the ability of human umbilical cord mesenchymal stem cells to support hematopoiesis in vitro. Mol. Med. Rep. 6, 827–832.
Suzuki, N., Koussevitzky, S., Mittler, R., Miller, G., 2012. ROS and redox signalling in the response of plants to abiotic stress. Plant Cell Environ. 35, 259–270.
Toyokuni, S., 2006. Novel aspects of oxidative stress-associated carcinogenesis. Antioxid. Redox Signal. 8, 1373–1377.
Wang, H., Tang, X., Sha, J., Chen, H., Sun, T., Wang, Y., 2015. The reproductive toxicity on the rotifer *Brachionus plicatilis* induced by BDE-47 and studies on the effective mechanism based on antioxidant defense system changes. Chemosphere 135, 129–137.
Wen, B., Zhou, R., Feng, Q., Wang, Q., Wang, J., Liu, S., 2014. IQuant: an automated pipeline for quantitative proteomics based upon isobaric tags. Proteomics 14, 2280–2285.
Woo, R.A., Poon, R.Y., 2004. Activated oncogenes promote and cooperate with chromosomal instability for neoplastic transformation. Genes Dev. 18, 1317–1330.
Wu, K., Xu, X., Liu, J., Guo, Y., Li, Y., Huo, X., 2010. Polybrominated diphenyl ethers in umbilical cord blood and relevant factors in neonates from Guiyu, China. Environ. Sci. Technol. 44, 813–819.
Xu, X., Yekeen, T.A., Xiao, Q., Wang, Y., Lu, F., Huo, X., 2013. Placental IGF-1 and IGFBP-3 expression correlate with umbilical cord blood PAH and PBDE levels from prenatal exposure to electronic waste. Environ. Pollut. 182, 63–69.
Xu, X., Liu, J., Zeng, X., Lu, F., Chen, A., Huo, X., 2014. Elevated serum polybrominated diphenyl ethers and alteration of thyroid hormones in children from Guiyu, China. PLoS ONE 9, e113699.
Xu, L., Huo, X., Zhang, Y., Li, W., Zhang, J., Xu, X., 2015. Polybrominated diphenyl ethers in human placenta associated with neonatal physiological development at a typical e-waste recycling area in China. Environ. Pollut. 196, 414–422.
Xu, L., Ge, J., Huo, X., Zhang, Y., Lau, A.T., Xu, X., 2016a. Differential proteomic expression of human placenta and fetal development following e-waste lead and cadmium exposure in utero. Sci. Total Environ. 550, 1163–1170.
Xu, Y.M., Wu, D.D., Zheng, W., Yu, F.Y., Yang, F., Yao, Y., Zhou, Y., Ching, Y.P., Lau, A.T., 2016b. Proteome profiling of cadmium-induced apoptosis by antibody array analyses in human bronchial epithelial cells. Oncotarget 7, 6146–6158.
Yu, K., He, Y., Yeung, L.W., Lam, P.K., Wu, R.S., Zhou, B., 2008. DE-71-induced apoptosis involving intracellular calcium and the Bax-mitochondria-caspase protease pathway in human neuroblastoma cells in vitro. Toxicol. Sci. 104, 341–351.
Zeng, H.L., Qin, Y.L., Chen, H.Z., Bu, Q.Q., Li, Y., Zhong, Q., Han, X.A., Chen, J., Yu, P.X., Liu, G.X., 2014. Effects of nicotine on proliferation and survival in human umbilical cord mesenchymal stem cells. J. Biochem. Mol. Toxicol. 28, 181–189.
Zhang, W., Liu, Y., Zhang, H., Dai, J., 2012. Proteomic analysis of male zebrafish livers chronically exposed to perfluorononanoic acid. Environ. Int. 42, 20–30.
Zhang, S., Kuang, G., Zhao, G., Wu, X., Zhang, C., Lei, R., Xia, T., Chen, J., Wang, Z., Ma, R., Li, B., Yang, L., Wang, A., 2013. Involvement of the mitochondrial p53 pathway in PBDE-47-induced SH-SY5Y cells apoptosis and its underlying activation mechanism. Food Chem. Toxicol. 62, 699–706.
Zhang, S., Xu, X., Wu, Y., Ge, J., Li, W., Huo, X., 2014. Polybrominated diphenyl ethers in residential and agricultural soils from an electronic waste polluted region in south china: distribution, compositional profile, and sources. Chemosphere 102, 55–60.
Zhang, W., Liu, K., Li, J., Liang, J., Lin, K., 2015. Impacts of BDE209 addition on Pb uptake, subcellular partitioning and gene toxicity in earthworm (Eisenia fetida). J. Hazard. Mater. 300, 737–744.
Zhao, A., Liu, H., Zhang, A., Wang, X., Zhang, H., Wang, H., 2011. Effect of BDE-209 on glutathione system in *Carassius auratus*. Environ. Toxicol. Pharmacol. 32, 35–39.
Zhao, Y., Ruan, X., Li, Y., Yan, M., Qin, Z., 2013. Polybrominated diphenyl ethers (PBDEs) in aborted human fetuses and placental transfer during the first trimester of pregnancy. Environ. Sci. Technol. 47, 5939–5946.
Zhao, Y., Liu, P., Wang, J., Xiao, X., Meng, X., Zhang, Y., 2016. Umbilical cord blood PBDEs concentrations are associated with placental DNA methylation. Environ. Int. 97, 1–6.
Zheng, C.F., Guan, K.L., 1993. Properties of MEKs, the kinases that phosphorylate and activate the extracellular signal-regulated kinases. J. Biol. Chem. 268, 23933–23939.
Zheng, J., He, C.T., Chen, S.J., Yan, X., Guo, M.N., Wang, M.H., Yu, Y.J., Yang, Z.Y., Mai, B.X., 2017. Disruption of thyroid hormone (TH) levels and TH-regulated gene expression by polybrominated diphenyl ethers (PBDEs), polychlorinated biphenyls (PCBs), and hydroxylated PCBs in e-waste recycling workers. Environ. Int. 102, 138–144.
Zhu, M., Dai, S., McClung, S., Yan, X., Chen, S., 2009. Functional differentiation of *Brassica napus* guard cells and mesophyll cells revealed by comparative proteomics. Mol. Cell. Proteomics 8, 752–766.